ELSEVIER

Chemical Geology 138 (1997) 257–271

CHEMICAL GEOLOGY
INCLUDING
ISOTOPE GEOSCIENCE

Partitioning of high field-strength and rare-earth elements between amphibole and quartz-dioritic to tonalitic melts: an experimental study

M. Klein [a,*], H.-G. Stosch [b], H.A. Seck [a]

[a] *Institut für Mineralogie und Geochemie der Universität zu Köln, Zülpicher Str. 49, 50674, Köln, Germany*
[b] *Institut für Petrographie und Geochemie der Universität Karlsruhe, Kaiserstr. 12, 76131, Karlsruhe, Germany*

Received 10 September 1996; accepted 20 February 1997

Abstract

The knowledge of rare-earth element (REE) and high field-strength element (HFSE) partitioning between minerals such as amphibole, pyroxenes or garnet and tonalitic liquids is essential to understand where and how tonalitic melts are generated. In this paper we present the results of trace-element partitioning studies between amphibole and quartz-dioritic to tonalitic liquids which have been conducted at 1 GPa and temperatures of 800°C, 850°C, and 900°C. Amphiboles crystallized from tonalitic liquids are nearly homogeneous, indicating that equilibrium has been closely attained. Henry's Law behaviour was confirmed for trace-element concentrations ranging from a few ppm as in natural systems up to doping levels of 0.5 wt.%. Partition coefficients (D) for the REE on the M4-site and of Ti, Zr and Hf on the M2-site of the amphibole structure can be fitted to parabolas, using the equation of Blundy and Wood (1994). Parabolas for all isovalent series of cations have the same shape in the temperature range investigated. The maxima of the parabolas for the REE defining the size of the unstrained site r_0 lie at Dy. At 1 GPa partition coefficients $D^{\mathrm{Amph/L}}$ for Dy range from 1.77 at 900°C to 2.68 at 800°C. $D^{\mathrm{Amph/L}}$ partition coefficients of Nb and Ta are identical within error limits. From this observation, together with the coincidence of their ionic radii with fitted radii of r_0 for the M2-site, it is concluded that partition coefficients of Nb and Ta plot close to the peak of the parabola for the pentavalent cations. From a comparison of the fitted parabola parameters of the REE for amphibole and clinopyroxene it is inferred that at fixed conditions the amphibole/clinopyroxene partition coefficients $D^{\mathrm{Cpx/Amph}}$ for all REE have to be constant.

The partition coefficients of the cations investigated in this study correlate negatively with the degree of depolymerisation in the melt expressed as the ratio of nonbridging oxygens to the number of tetrahedrons (NBO/T). Logarithms of partition coefficients normalized to the degree of depolymerisation define a linear function when plotted versus reciprocal temperature. By means of the fitted parabola parameters, straight-line relationships between D_{REE} and D_{Ca} as well as D_{REE} and D_{Ti} can be calculated. The predicted correlations agree very well with the experimentally determined data.

Keywords: Partition coefficients; Experimental geochemistry; Amphibole; Quartz-diorite; Tonalite; Rare earth elements

* Corresponding author. FAX: 0221-470 5199; E-mail: KLEINM@geocip.geo.uni-Koeln.de.

PII S0009-2541(97)00019-3

1. Introduction

Recent experimental studies have demonstrated that tonalites, trondhjemites and granodiorites, which are widespread constituents of the continental crust, may form by partial melting of amphibolites over a wide range of pressures and temperatures (0.1–3.2 GPa and 800–1100°C) appropriate for the conditions of the lower continental crust and of the subducted oceanic slab (Beard and Lofgren, 1991; Rapp et al., 1991; Rushmer, 1991; Winther and Newton, 1991; Wolf and Wyllie, 1994; Rapp, 1995; Rapp and Watson, 1995). Many tonalites from Archaean greenstone-belts and other felsic rocks present in modern active continental margins have steep negative REE slopes with chondrite-normalized La/Yb ratios ranging from 10 to 100 (Rudnick and Taylor, 1986; Wedepohl et al., 1991).

Modelling these steep REE patterns requires reliable sets of partition coefficients between the residual minerals and the melt. Amphibole is one of the potential major residual phases. Past experimental studies have focused on amphiboles coexisting with basanitic (Adam and Green, 1994; LaTourette et al., 1995), andesitic (Nicholls and Harris, 1980; Green and Pearson, 1985; Brenan et al., 1995) and carbonatitic melts (Sweeney et al., 1992; Green et al., 1992) but data available for tonalite melts are rare (Arth and Barker, 1976). In this paper we present new experimentally determined partition coefficients of 10 REE and the high field-strength elements (HFSE) Nb, Ta, Hf, Zr, and Ti for pargasitic hornblendes in equilibrium with quartz-dioritic to tonalitic melts. The large number of elements allows an investigation of the crystal chemical and melt structural controls on trace-element partitioning.

2. Experimental methods

2.1. Partitioning experiments

Experiments were carried out in a piston–cylinder apparatus of the type described by Johannes (1973) at 1 GPa and 800°C, 850°C, 900°C. Throughout this study the piston-in technique was used. Furnace assemblies had a diameter of 22 mm and were made with fluorite sleeves and a combination of soft-fired pyrophyllite and fluorite inserts. The pressure was calibrated using the pressure dependency of the reaction *fayalite + quartz ↔ ferrosilite* (Bohlen et al., 1980). The results of several experiments conducted at different pressures with a mix of fayalite, quartz, and ferrosilite required a −7.5% correction to be applied to measured pressures. Temperatures read from Pt_{100}–$Pt_{90}Rh_{10}$ thermocouples are estimated to be accurate to within 5°C. No pressure correction on the EMF was applied. Oxygen fugacity within the furnace assemblies was found to lie between the Ni–NiO and quartz–magnetite–fayalite buffers. Runs lasted from 40 to 85 h.

A natural quartz-diorite (T1, composition see Table 1) from the Central-Alpine Bergell intrusion (Val Melirolo, Italian Alps) was used as starting material. Rock powders were ground to sizes of ≤ 2 μm. For electron microprobe (EMP) measurements, 0.5 wt.% of the elements to be studied were added as oxides. In order to minimize changes in bulk composition and avoid mutual analytical interferences, no more than two trace-element oxides were added to each experimental charge. Powders were homogenized by grinding under acetone with an agate mortar. After drying the powder at 200°C, 10–20 mg of each batch and a quantity of H_2O equivalent to 7.5 wt.% of the charge were loaded into gold-capsules

Table 1
Bulk composition of sample T1 (major- and trace-element composition measured by XRF and ICP–AES, respectively, are given in wt.% and ppm)

Oxide	wt.%	Element	ppm
SiO_2	57.9	La	73.9
TiO_2	0.75	Ce	127
Al_2O_3	17.1	Nd	44.4
Fe_2O_3	2.35	Sm	6.95
FeO	4.59	Eu	1.26
MnO	0.14	Gd	4.16
MgO	3.85	Dy	4.74
CaO	7.00	Er	2.39
K_2O	2.22	Yb	2.55
Na_2O	3.01	Lu	0.37
P_2O_5	0.20		
CO_2	0.04		
Sum	99.12		

which were sealed by welding. Undoped experiments were carried out to check for Henry's Law behaviour.

The samples were heated to 50°C above the liquidus (1000°C) to allow the melt to homogenize. After 30 min the temperatures were decreased to the run temperature over a period of about half an hour.

2.2. Analytical techniques

Run products were analysed for major and minor elements with a Cameca Camebax Microbeam electron microprobe using various mineral-, oxide-, and REE-fluoride standards for calibration. Counting times were 5 s for the alkalis, 10 s for all other major and minor elements, and 30 s for trace elements added. The beam was focused to a diameter of 2 μm at an accelerating voltage of 15 kV for major and 25 kV for trace elements. Operating currents were 10 and 100 nA for major and trace elements, respectively. Glasses were measured by beam scanning across an area of at least 400 μm^2 to minimize loss of the alkalis. Correction of X-ray intensities for deadtime, background, and matrix effects was made using the Cameca ZAF-routine. Reported concentrations for each phase were averaged from 15 analyses at different grains within the same sample.

Following the method of McKay and Seymour (1982), partition coefficients were determined as the ratios of the net intensities of the pertinent X-ray lines in amphibole and glass. This technique avoids instrumental drifts, due to simultaneous measurement of peak and background. In addition to their method, net intensities were matrix-corrected using the equations of Philbert (1963), Berger and Seltzer (1964), Reed (1965), Duncumb and Shields (1966), Duncumb and Reed (1968), Heinrich (1969) and Yakowitz et al. (1973); all cited in Reed (1975). These calculations show that matrix corrections are necessary for Nb and Zr (Klein, 1995), whereas for all other elements the error due to the lack of matrix corrections is less than analytical and experimental errors.

REE-contents of amphiboles and glasses of the undoped sample were measured with a Cameca IMS-3f ion microprobe at the Woods Hole Oceanographic Institution. Operating conditions were as described by Shimzu and LeRoex (1986), Johnson et al. (1990) and Sisson (1991). A glass produced by D. Dingwell at the Bayerisches Geoinstitut Bayreuth from sample T1 and analysed by ICP-AES was used as an external standard to check for the accuracy of the measurements. Homogeneity of the glass was achieved by stirring the melt. The trace-element composition of the glass is given in Table 1. Due to their low concentrations in amphibole, Nb and Ta could not be analysed with sufficient precision using electron microprobe techniques. For this reason, they were measured with a Cameca IMS-4f ion microprobe at the Department of Geology and Geophysics in Edinburgh. Operating conditions were as described by Hinton and Harte (1995) and Witt-Eickschen and Harte (1994). Corrections were made for mass interferences of ^{149}SmO on ^{165}Ho and ^{165}HoO on ^{181}Ta. For Sm, three independent $D^{\mathrm{Amph/L}}$ values were obtained in this study, i.e. by electron microprobe in

Table 2
Experimental run conditions; chemical modes are calculated by least-squares regression

Doped oxides	T (°C)	Run duration (h)	Glass (wt.%)	Amph (wt.%)
HfO_2, La_2O_3	900	85	81	18
CeO_2, Eu_2O_3	900	85	81	18
Nd_2O_3, Er_2O_3	900	65	82	17
Sm_2O_3, Yb_2O_3	900	68	80	19
Gd_2O_2, ZrO_2	900	85	85	14
Dy_2O_3, Lu_2O_3	900	70	81	18
Nb_2O_5, Ta_2O_5	900	70	83	16
HfO_2, La_2O_3	850	85	71	29
CeO_2, Eu_2O_3	850	70	73	26
Nd_2O_3, Er_2O_3	850	70	73	26
Sm_2O_3, Yb_2O_3	850	70	74	26
Gd_2O_2, ZrO_2	850	70	72	28
Dy_2O_3, Lu_2O_3	850	85	70	29
Nb_2O_5, Ta_2O_5	850	85	73	26
HfO_2, La_2O_3	800	60	60	41
CeO_2, Eu_2O_3	800	61	61	39
Nd_2O_3, Er_2O_3	800	61	61	39
Sm_2O_3, Yb_2O_3	800	62	62	38
Gd_2O_2, ZrO_2	800	60	60	40
Dy_2O_3, Lu_2O_3	800	58	58	42
Nb_2O_5, Ta_2O_5	800	59	59	40
None	850	70	74	24

the system doped with Sm and by ionprobe in the laboratories at Woods Hole and Edinburgh from samples containing Sm in natural concentrations. All these data agree within analytical error limits, indicating that the results produced in these three laboratories are comparable.

Table 3
Averages of 15 EMP analyses of glasses and amphiboles in tonalite experiments with doped samples

	La^{3+} [a] + Hf^{4+} [b]	Ce^{4+} [a] + Eu^{3+} [b]	Nd^{3+} [a] + Er^{3+} [b]	Sm^{3+} [a] + Yb^{3+} [b]	Gd^{3+} [a] + Zr^{4+} [b]	Dy^{3+} [a] + Lu^{3+} [b]	Nb^{5+} [a] + Ta^{5+} [b]
Analyses for experiments at 900°C, 1 GPa, $n = 15$							
Amphiboles:							
SiO_2	43.2(4)	43.5(5)	43.6(9)	43.4(6)	43.3(8)	42.9(4)	42.7(4)
TiO_2	1.44(9)	1.50(9)	1.40(10)	1.57(11)	1.49(9)	1.32(5)	1.42(10)
Al_2O_3	12.4(4)	12.2(4)	12.3(5)	12.4(4)	12.4(4)	12.6(3)	12.23(15)
FeO	11.2(3)	11.7(3)	11.3(2)	10.9(3)	11.3(3)	11.5(3)	10.9(3)
MnO	0.15(4)	0.16(5)	0.18(3)	0.14(6)	0.13(6)	0.13(4)	0.11(5)
MgO	14.0(3)	13.4(4)	13.23(19)	13.5(3)	13.7(4)	13.44(18)	14.4(2)
CaO	11.0(2)	10.93(14)	10.9(2)	10.95(13)	10.92(15)	10.85(14)	11.43(17)
K_2O	1.08(7)	1.09(8)	1.08(10)	1.03(4)	1.05(8)	1.05(5)	1.05(7)
Na_2O	1.91(10)	1.97(8)	1.94(8)	1.94(10)	1.78(13)	2.02(10)	1.94(14)
H_2O	1.99	1.94	1.97	2.01	1.98	1.99	1.98
Oxide [a]	0.09(2)	0.16(1)	0.31(5)	0.64(4)	0.48(3)	0.87(5)	0.19(2)
Oxide [b]	0.19(1)	0.48(2)	0.68(4)	0.55(2)	0.11(1)	0.51(2)	0.11(1)
Sum	98.65	99.03	98.89	99.03	98.64	99.18	98.46
Glasses:							
SiO_2	61.1(6)	61.1(6)	61.0(6)	61.8(5)	60.5(8)	61.1(8)	60.9(9)
TiO_2	0.64(4)	0.60(5)	0.56(6)	0.61(5)	0.70(4)	0.56(5)	0.69(3)
Al_2O_3	17.7(3)	17.21(14)	17.6(2)	17.3(2)	17.3(3)	17.8(3)	17.5(5)
FeO	5.1(3)	5.5(2)	5.8(2)	5.6(2)	5.7(2)	5.2(3)	5.33(18)
MnO	0.14(4)	0.16(4)	0.15(6)	0.14(3)	0.14(5)	0.12(6)	0.11(4)
MgO	2.35(15)	2.12(16)	2.63(16)	2.06(10)	2.63(10)	2.38(8)	2.47(17)
CaO	6.12(14)	6.4(14)	5.9(2)	6.14(10)	7.00(10)	6.28(15)	6.28(17)
K_2O	2.31(14)	2.54(10)	2.06(14)	2.09(10)	2.30(8)	2.29(17)	2.43(11)
Na_2O	3.41(11)	3.18(6)	3.30(7)	3.24(11)	3.02(11)	3.3(2)	3.24(15)
Oxide [a]	0.71(8)	0.67(7)	0.49(5)	0.47(2)	0.32(1)	0.49(3)	0.69(1)
Oxide [b]	0.45(3)	0.44(1)	0.46(1)	0.48(1)	0.43(3)	0.48(1)	0.41(2)
Sum	100.03	99.92	99.95	99.93	100.04	100.00	100.05
Analyses for experiments at 850°C, 1 GPa, $n = 15$							
Amphiboles:							
SiO_2	42.0(1.0)	41.9(1.1)	41.8(4)	41.1(8)	41.4(9)	41.6(1.0)	41.6(1.0)
TiO_2	1.5(2)	1.68(19)	1.66(15)	1.51(14)	1.3(2)	1.6(2)	1.36(9)
Al_2O_3	13.1(7)	13.0(6)	12.5(3)	12.7(6)	13.4(4)	13.6(3)	13.13(13)
FeO	13.4(5)	13.7(8)	13.6(4)	13.1(3)	13.3(8)	13.4(7)	12.9(2)
MnO	0.24(6)	0.11(6)	0.16(5)	0.18(8)	0.20(6)	0.20(4)	0.14(3)
MgO	13.0(6)	12.6(6)	12.9(2)	12.9(3)	12.4(9)	12.5(6)	12.5(3)
CaO	10.6(4)	10.5(5)	10.6(3)	10.8(3)	10.7(5)	10.3(6)	11.40(13)
K_2O	1.19(11)	1.07(3)	0.95(14)	0.95(14)	1.07(11)	0.99(8)	1.10(9)
Na_2O	1.7(2)	1.94(13)	1.80(8)	1.72(8)	1.7(2)	2.00(14)	1.84(9)
H_2O	1.98	1.98	1.97	1.97	1.90	2.02	1.99
Oxide [a]	0.13(3)	0.15(2)	0.64(6)	0.88(8)	0.78(16)	1.16(6)	0.28(3)
Oxide [b]	0.34(3)	0.70(7)	0.64(2)	0.62(4)	0.31(2)	0.64(5)	0.25(2)
Sum	99.18	99.33	99.22	98.47	98.46	100.01	98.49

3. Homogeneity of the phases and Henry's Law behaviour

As shown by Adam et al. (1993), amphiboles crystallizing from melts are prone to compositional zoning or heterogeneities due to disequilibrium growth. Therefore, each run product—i.e. for seven runs carried out at each temperature—was carefully checked for homogeneity of the major elements in the phases as follows. At least one line profile was

Table 3 (continued)

	La^{3+} [a] + Hf^{4+} [b]	Ce^{4+} [a] + Eu^{3+} [b]	Nd^{3+} [a] + Er^{3+} [b]	Sm^{3+} [a] + Yb^{3+} [b]	Gd^{3+} [a] + Zr^{4+} [b]	Dy^{3+} [a] + Lu^{3+} [b]	Nb^{5+} [a] + Ta^{5+} [b]
Glasses:							
SiO_2	64.2(7)	64.0(1.2)	63.8(5)	63.6(7)	63.8(4)	63.9(7)	63.5(6)
TiO_2	0.47(3)	0.46(5)	0.51(4)	0.55(3)	0.42(4)	0.51(2)	0.47(4)
Al_2O_3	17.5(3)	18.0(4)	17.9(2)	17.8(4)	17.9(2)	18.4(2)	17.9(4)
FeO	4.14(17)	4.9(2)	4.71(16)	4.58(12)	4.3(2)	4.6(2)	4.62(18)
MnO	0.12(2)	0.09(3)	0.14(8)	0.14(3)	0.09(3)	0.12(4)	0.15(3)
MgO	0.71(7)	1.21(9)	1.09(10)	1.44(9)	1.04(7)	0.71(12)	1.13(12)
CaO	5.74(12)	5.68(14)	5.65(15)	5.72(11)	5.58(11)	5.17(14)	5.20(11)
K_2O	2.33(9)	1.58(14)	1.99(14)	2.09(12)	2.29(11)	2.32(7)	1.97(11)
Na_2O	3.64(9)	3.34(6)	3.30(18)	3.29(9)	3.39(11)	3.41(7)	3.42(13)
Oxide [a]	0.71(11)	0.34(3)	0.63(4)	0.48(4)	0.41(7)	0.49(2)	0.81(8)
Oxide [b]	0.52(3)	0.43(5)	0.32(1)	0.35(2)	0.76(5)	0.40(2)	0.79(8)
Sum	100.08	100.03	100.04	100.04	99.98	100.03	99.96
Analyses for experiments at 800°C, 1 GPa, $n = 15$							
Amphiboles:							
SiO_2	41.4(9)	41.5(4)	41.2(7)	41.0(1.2)	41.8(7)	42.0(7)	42.2(9)
TiO_2	1.5(2)	1.53(15)	1.54(17)	1.9(2)	1.47(19)	1.4(2)	1.17(16)
Al_2O_3	13.6(9)	13.5(4)	13.6(5)	13.3(7)	13.3(1.3)	13.2(9)	13.7(8)
FeO	14.4(8)	14.7(3)	14.3(5)	14.2(9)	14.0(1.1)	14.3(7)	14.8(7)
MnO	0.28(2)	0.20(2)	0.15(6)	0.20(9)	0.25(7)	0.25(4)	0.24(7)
MgO	10.1(2)	10.3(4)	10.46(17)	10.9(1.0)	10.2(6)	10.4(7)	10.1(3)
CaO	11.0(4)	10.7(3)	10.9(3)	11.0(3)	11.0(3)	10.5(2)	11.2(3)
K_2O	1.38(17)	0.88(10)	0.90(11)	0.92(10)	1.1(2)	1.13(14)	1.04(13)
Na_2O	1.8(2)	2.10(11)	1.82(13)	1.9(2)	1.7(2)	1.82(19)	1.8(2)
H_2O	2.04	1.98	1.97	1.97	1.97	2.01	2.00
Oxide [a]	0.30(5)	0.57(6)	0.52(4)	0.86(8)	1.14(12)	1.26(11)	0.23(3)
Oxide [b]	0.51(7)	0.82(9)	0.99(8)	0.88(5)	0.49(14)	0.89(16)	0.26(5)
Sum	98.31	98.68	98.25	99.03	98.42	99.16	98.74
Glasses:							
SiO_2	68.0(1.0)	67.8(1.0)	67.7(6)	67.9(9)	67.9(5)	68.7(7)	68.4(5)
TiO_2	0.27(3)	0.36(8)	0.33(4)	0.32(7)	0.33(3)	0.25(2)	0.39(3)
Al_2O_3	17.1(3)	16.8(3)	17.80(13)	17.52(11)	17.65(13)	17.4(3)	17.2(4)
FeO	2.2(2)	2.3(2)	2.2(2)	2.5(2)	2.1(2)	1.95(10)	2.07(18)
MnO	0.08(2)	0.08(3)	0.12(6)	0.11(5)	0.12(3)	0.06(3)	0.08(3)
MgO	0.46(7)	0.78(12)	0.66(7)	0.48(14)	0.60(8)	0.35(3)	0.54(10)
CaO	4.28(11)	4.4(2)	4.74(13)	4.8(2)	4.69(11)	4.33(5)	4.28(10)
K_2O	2.62(16)	2.51(9)	2.21(14)	2.07(15)	1.99(14)	2.26(11)	1.98(10)
Na_2O	3.7(2)	3.51(15)	3.43(11)	3.4(2)	3.40(19)	3.70(10)	3.84(8)
Oxide [a]	0.81(14)	0.78(7)	0.43(3)	0.43(4)	0.48(4)	0.47(3)	0.59(5)
Oxide [b]	0.54(6)	0.62(6)	0.40(3)	0.42(2)	0.72(15)	0.51(7)	0.68(9)
Sum	100.06	99.94	100.02	99.95	99.98	99.98	100.05

Trace-element concentrations of the amphiboles were recalculated from the experimental glass compositions and the *D*-values as determined separately. Glass analyses were recalculated to a H_2O-free composition.

measured across each phase. Moreover, at least fifteen analyses were carried out on different spots on various grains of each phase. No zonations or inhomogeneities of major elements in amphiboles or quenched melts were detected, indicating that disequilibrium growth during our experiments is unlikely.

For an additional test of trace-element homogeneity in each phase, a method of Boyd et al. (1969) was applied. These authors proposed that a phase can be considered homogeneous with respect to a particular element, if the ratio $K = s'/\sqrt{N}$ is less than 3. N is the average number of counts of all analyses of the phase of interest and s' is the standard deviation. Run products for which K exceeded the value of 3 in any phase were disregarded.

To confirm that Henry's Law is fulfilled for doping levels of 0.5 wt.%, we have plotted the results from the doped and undoped runs in Fig. 1. The data agree within analytical error limits for each element, thus indicating that Henry's Law is obeyed in our experiments.

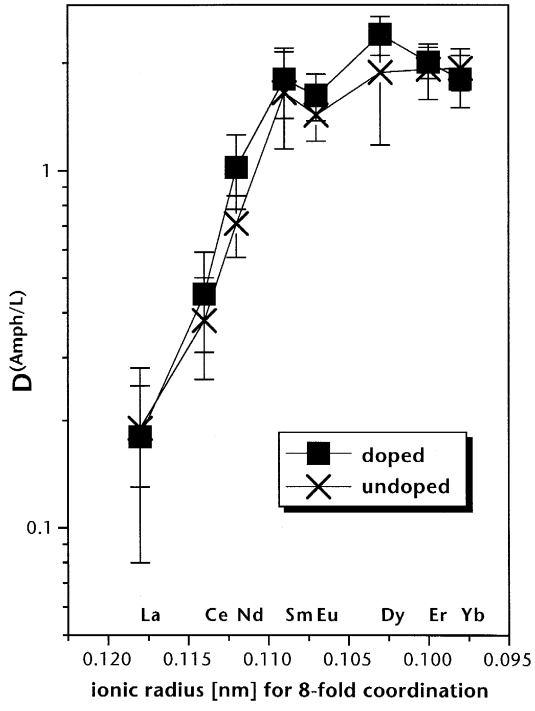

Fig. 1. Partition coefficients of REE for amphiboles synthesized at 850°C and 1 GPa with doped (measured with EMP) and undoped (SIMS analyses) samples.

4. Run products and phase compositions

Run products are composed of silicate melts and amphiboles with crystal sizes ranging from 30 μm up to 70 μm. No other phases were produced. According to the classification of Streckeisen and LeMaitre (1979) the composition of the melt is quartz-dioritic at 900°C and tonalitic at 850°C and 800°C if CIPW norms are taken as modes. The modes of the phases in terms of wt.% as calculated from major-element mass balance are shown in Table 2. The modal proportion of amphibole increased from 18 wt.% up to 40 wt.% in the temperature range from 900°C down to 800°C. The glasses are clear in all runs and no quench crystallization is observed.

The compositions of the amphiboles and the melts recalculated to 100 wt.% on a H_2O-free basis are listed in Table 3. The Mg# $[Mg/(Mg + \Sigma Fe)]$ of the crystals increase with temperature from 0.55 to 0.70. That is, the composition of the calcic amphiboles changes from ferroan pargasitic hornblendes to pargasitic hornblendes according to the amphibole classification of Leake (1978). As shown in Table 3 the Ti-, Na-, K-, Ca-, and Si-contents of the amphiboles do not change with temperature. Trace-element concentrations of the amphiboles given in Table 3 were recalculated from the experimental glass compositions and the D values.

The SiO_2- and Na_2O-concentrations of the glasses increase from 54 to 61 wt.% and from 2.8 to 3.2 wt.%, respectively, with a concomitant depletion of MgO, FeO, CaO, and TiO_2 if the degree of crystallization is increased, whereas the Al_2O_3- and the K_2O-contents do not change.

5. Partition coefficients

5.1. Correlation between partition coefficients and ionic radii

Partition coefficients obtained in this study are presented in Table 4. The curves in Fig. 2, relating the partition coefficients D_i to the ionic radii r_i of the pertinent elements, are calculated from least-

squares fits using the thermodynamically derived expression presented by Blundy and Wood (1994):

$$D_i = D_0 \exp\left\{ -\frac{4\pi E N_A}{RT}\left[\frac{r_0}{2}(r_i - r_0)^2 + \frac{1}{3}(r_i - r_0)^3\right]\right\} \quad (1)$$

where D_0 is the partition coefficient corresponding to the optimal radius r_0 of a given crystallographic site; E is Young's modulus, N_A Avogadro's number, R the gas constant and T the absolute temperature. This relationship accounts for the strain associated with placing a cation on a particular crystallographic site when the radius of the cation differs from the optimal radius for that site. The model assumes that the character of the chemical bonding in the crystals is ionic and it predicts that the partition coefficients for an isovalent series of cations substituting on the same site falls on a parabola, when plotted as a logarithmic function of ionic radius. The maxima of the parabolas define the partition coefficient D_0 which corresponds to the best-fit radius r_0 for that site, i.e. $D_i = D_0$ if $r_i = r_0$. Young's modulus E for a given site determines the opening of the parabola; that is, the larger E the narrower is the parabola.

The following discussion is based upon the assumption that the REE follow Ca into the distorted M4-site with 8-fold coordination and that the tetra- and pentavalent cations such as Hf, Zr, Nb, and Ta preferentially occupy the M2-site with 6-fold coordination, which is commonly assumed for Ti. Using the ionic radii of Shannon and Prewitt (1968) we calculate values of r_0, D_0, and E for each run-tem-

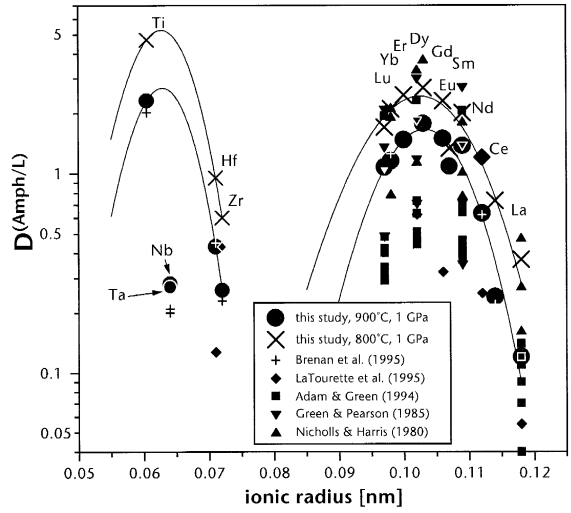

Fig. 2. Partition coefficients for amphiboles. The curves are calculated using the relationship of Blundy and Wood (1994). Experimental conditions of the data of the literature: Adam and Green (1994): 1000°C-1100°C, 0.5-2 GPa; Brenan et al. (1995): 1000°C, 1.5 GPa; LaTourette et al. (1995): 1100°C, 1.5 GPa; Nicholls and Harris (1980): 900°C-1020°C, 1 GPa; Green and Pearson (1985): 900°C-1050°C, 0.75-2 GPa.

Table 4
Amphibole-melt partition coefficients determined with EMP and SIMS

Element	900°C, doped	850°C, doped	850°C, undoped	800°C, undoped
La	0.12 ± 0.03	0.18 ± 0.05	0.190 ± 0.029	0.37 ± 0.09
Ce	0.24 ± 0.03	0.45 ± 0.07	0.38 ± 0.06	0.73 ± 0.10
Nd	0.63 ± 0.12	1.02 ± 0.12	0.71 ± 0.07	1.20 ± 0.13
Sm	1.37 ± 0.11	1.83 ± 0.22	1.65 ± 0.23	2.01 ± 0.25
Eu	1.08 ± 0.05	1.62 ± 0.24	1.43 ± 0.11	1.33 ± 0.19
Gd	1.49 ± 0.11	1.9 ± 0.5		2.3 ± 0.3
Dy	1.77 ± 0.15	2.37 ± 0.16	1.88 ± 0.35	2.68 ± 0.3
Er	1.47 ± 0.09	2.01 ± 0.10	1.92 ± 0.17	2.47 ± 0.26
Yb	1.15 ± 0.05	1.77 ± 0.15	1.93 ± 0.13	2.10 ± 0.15
Lu	1.07 ± 0.05	1.61 ± 0.16		1.7 ± 0.4
Zr	0.26 ± 0.03	0.42 ± 0.04		0.68 ± 0.24
Hf	0.43 ± 0.04	0.66 ± 0.07		0.95 ± 0.17
Ti	2.32 ± 0.22	3.2 ± 0.4	2.7 ± 0.5	4.7 ± 0.7
Nb	0.28 ± 0.03	0.34 ± 0.05		0.39 ± 0.06
Ta	0.27 ± 0.03	0.32 ± 0.04		0.38 ± 0.09

Errors represent 1σ uncertainties calculated by propagating the standard deviation of the mean.

perature. The curves for the REE in Fig. 2 display distinct maxima at Dy. The shape of the parabolas for each site remains constant at all temperatures studied. However, with r_0 being constant, D_0 is shifted to lower values as temperature is raised from 800°C to 900°C. Note that this is not an effect of temperature alone. D_0 also depends on concentration variables which themselves are temperature dependent.

The slopes of the parabolas are steeper for tetravalent cations than for the trivalent REE. This is consistent with the observation of Hazen and Finger (1979) who showed that the bulk moduli of lattice sites, which are proportional to Young's modulus E, increase with decreasing volume of a site and the enhancing charge of the cations occupying that site. The difference in the partition coefficients of Zr and Hf was previously reported by Brenan et al. (1995) and LaTourette et al. (1995). It is a result of the large value of Young's modulus E of the M2-site and the concomitant steep slope of the branches of the parabola. The ionic radii of Nb and Ta are identical (Fig. 2) and also very close to the fitted value r_0 for the M2-site; hence, their partition coefficients plot near the peak of the parabola (see Table 5).

Table 5 also compares the fitted values of r_0, D_0, and E of this study with data reported in the literature. In spite of the variation in run conditions and in phase compositions, the fitted site radii r_0 agree very well within error limits for each site. The values for

Table 5
Comparison of lattice site parameters for amphiboles estimated from partitioning data of this and other studies with values determined by X-ray diffraction; 1σ-errors are calculated from the variance–covariance matrix following the method of Deming (1964)

T (°C)	P (GPa)	Site	Charge	r_0 (nm)	E (GPa)	D_0	System	Ref.
800	1	M4	3	0.103 ± 0.001	170 ± 60	2.66 ± 0.19	tonalite	1
850	1	M4	3	0.103 ± 0.001	250 ± 60	2.29 ± 0.10	tonalite	1
900	1	M4	3	0.103 ± 0.001	300 ± 80	1.75 ± 0.10	tonalite	1
900	1	M4	3	0.103 ± 0.007	110 ± 80	1.7 ± 0.8	andesite	2
1000	0.5	M4	3	0.104	240	0.80	basanite	3
1000	1.5	M4	3	0.099 ± 0.003	200 ± 80	1.3 ± 0.2	andesite	4
1050	2	M4	3	0.103	200	0.45	basanite	3
1050	2	M4	3	0.104	250	0.49	basanite	3
1050	1.5	M4	3	0.104	190	0.54	basanite	3
1100	2	M4	3	0.104	160	0.57	basanite	3
1100	1.5	M4	3	0.103	390	0.604	basanite	5
800	1	M2	4	0.061	530	4.70	tonalite	1
850	1	M2	4	0.063	850	3.56	tonalite	1
900	1	M2	4	0.061	640	2.35	tonalite	1
1100	1.5	M2	4	0.062	960	1.43	basanite	5
1000	1.5	M2	4	0.064 ± 0.001	1600 ± 150	3.5 ± 0.7	andesite	4
Data from structure refinements of pargasitic amphiboles of Comodi et al. (1991) at 0.0001 GPa								
		M4–O2		0.2403				6
		M4–O4		0.2322				6
		M4–O5		0.2655				6
		M4–O6		0.2588				6
		mean M4–O		0.2492				6
		M2–O1		0.2091				6
		M2–O2		0.2074				6
		M2–O4		0.2003				6
		mean M2–O		0.2056				6

References. 1: this study; 2: Green and Pearson, 1985; 3: Adam and Green, 1994; 4: Brenan et al., 1995; 5: LaTourette et al., 1995; 6: Comodi et al., 1991; r_0 determined for pargasite by structural refinement using X-ray diffraction data.

the M4-site and the M2-site correspond to the ionic radii of Dy ($r_{Dy} = 0.103$ nm for 8-fold coordination, after Shannon and Prewitt, 1968) and of Nb and Ta ($r_{Nb} = r_{Ta} = 0.064$ nm for 6-fold coordination, after Shannon and Prewitt, 1968), respectively.

The M4–O distance of 0.241 nm obtained from r_0 and an O^{2-}-radius of 0.138 nm (Shannon and Prewitt, 1968) matches the value of 0.240 nm for the M4-O2 bond length of the pargasite structure (Comodi et al., 1991). In a distorted polyhedron like M4 in which the M4–O5 and M4–O6 distances are much longer, an unstrained state is obviously maintained if the radius of the substituting cation meets the distance of the shorter bond lengths. This is also valid for the M2 polyhedron where the distance of 0.200 nm fitted by the experimental data of this study matches the value 0.200 nm for the M2–O4 bond length of the pargasite structure.

Although the relative differences in E are larger than those of r_0, values of E derived from data of this study and of the literature agree within error limits. An exception is the E-value of Brenan et al. (1995) for the M2-site which is much larger than the others. This may be due to the fact, that the amphiboles of the study of Brenan et al. (1995) are free of iron. The Young's modulus for the M2-site incorporating the tetravalent cations, is three times that of the M4-site which incorporates the REE. As mentioned previously, this is consistent with the observation of Hazen and Finger (1979).

Calculated partition coefficients D_0 of the unstrained sites show large variations within the investigated range of temperatures and melt compositions. The temperature dependence of D_0 applies to all cations of the pertinent isovalent suite because E and r_0 of amphibole are virtually unaffected by changes in P, T and X.

Also for clinopyroxenes, the radius r_0 and Young's modulus E of the M2-site were determined by non-linear least squares regressions from some experimentally determined REE partition coefficients of the literature (Hart and Dunn, 1993; Skulski et al., 1994; Hauri et al., 1994; Adam and Green, 1994). The data are presented in Table 6. In spite of the large variation of run conditions employed in these different studies, the values listed for r_0 (0.102 ± 0.001 nm) and E (270 ± 70 GPa) agree within error limits. The comparison of these data with those of the amphiboles ($r_0 = 0.103 \pm 0.001$ nm, $E = 240 \pm 70$ GPa) reveals no differences. Hence, also the exponential term in Eq. (1) is identical for amphiboles and clinopyroxenes at fixed temperature for each REE. This means that the parabolas for amphiboles and clinopyroxenes have identical shapes and division of Eq. (1) for clinopyroxenes by that for amphiboles (D^{Cpx}/D^{Amph}) leads to:

$$\frac{D_i^{Cpx/L}}{D_i^{Amph/L}} = \frac{D_0^{Cpx/L}}{D_0^{Amph/L}} \quad (2)$$

where i may be substituted by any REE. The right hand side of Eq. (2) is constant, indicating that the partition coefficients $D^{Cpx/Amph}$ are identical for all REE at fixed conditions. This is also reported by Witt-Eickschen and Harte (1994) and Chazot et al. (1996) in natural samples.

Table 6
Comparison of lattice parameters for clinopyroxenes estimated from partitioning data of this and other studies with values determined by X-ray diffraction; 1σ-errors are calculated from the variance–covariance matrix following the method of Deming (1964)

T (°C)	P (GPa)	Site	Charge	r_0 (nm)	E (GPa)	D_0	System	Ref.
1665	3	M2	3	0.105	400 ± 30		basalt	1
1380	3	M2	3	0.101	250 ± 50	0.45	basalt	2
1430	2.5	M2	3	0.100	240 ± 90	0.64	basalt	3
1405	1.7	M2	3	0.101	280 ± 60	0.45	basalt	3
1300	1	M2	3	0.102	310 ± 50	0.29	basalt	4
1235	1	M2	3	0.102	280 ± 50	1.17	basalt	4
1270	2.5	M2	3	0.102	220 ± 60	0.44	basalt	4
1200	2	M2	3	0.102	250 ± 40	0.55	basanite	5
1350	3	M2	3	0.104	170 ± 70	0.33	basanite	5

References. 1: Blundy and Wood, 1994; 2: Hart and Dunn, 1993; 3: Hauri et al., 1994; 4: Skulski et al., 1994; 5: Adam and Green, 1994.

5.2. Estimation of the Eu^{2+}/Eu^{3+} ratio

All REE curves displayed in Fig. 2 show negative Eu-anomalies which may be attributed to part of the Eu being divalent. For an estimation of the Eu^{2+}/Eu^{3+} ratio of the experiments of this study, we make use of the model of Blundy and Wood (1994), which allows us to calculate the partition coefficients of an isovalent series of cations. The parameters needed are the size of the unstrained lattice site r_0, the Young's Modulus E of this site, and one partition coefficient of this suite of isovalent cations. The partition coefficient of Eu^{3+} can be calculated using the fitted parameters for the REE. If we assume that Eu^{2+} also occupies the M4-site, it must plot on the same parabola as Ca having an r_0 value identical to the one of the REE. Table 5 suggests that Young's modulus for the data series of this study and the literature is independent of temperature and phase composition, at least within the range of the temperatures and bulk compositions listed. Using Young's modulus for the divalent cations studied by Brenan et al. (1995) and the Ca partition coefficient of this study, it is possible to calculate the parabola for the partition coefficients of the divalent cations at 800°C. Fig. 3 shows the curves for the trivalent and divalent cations on the M4-site with the calculated values $D^{Amph/L}$ for Eu^{3+} and Eu^{2+} at 800°C. These values together with the bulk partition coefficient of Eu observed for 800°C and 1 GPa, allow us to estimate the Eu^{2+}/Eu^{3+} ratio by mass balance calculations. According to this estimate, about 50% of Eu in the experiments of this study is divalent.

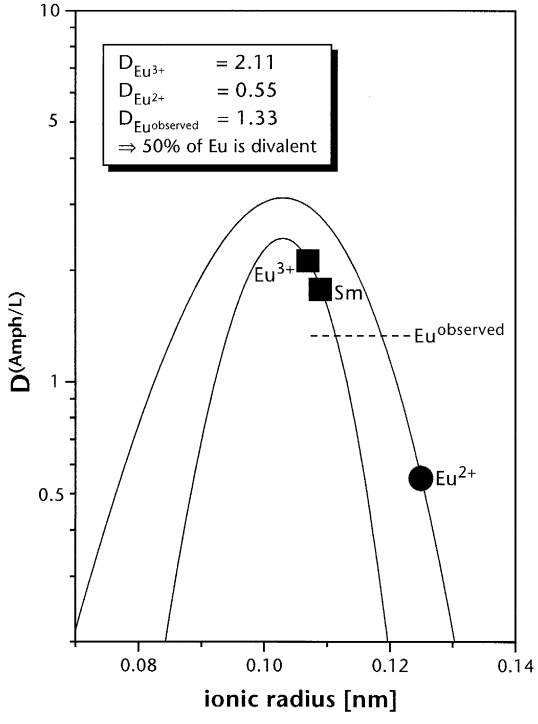

Fig. 3. Estimation of the Eu^{2+}-proportion from the calculated Onuma-curves (Blundy and Wood, 1994) for the divalent and trivalent cations.

5.3. Correlations between partition coefficients and temperature

Eq. (1) describes the temperature dependence of the partition coefficients in so far as it predicts the shape of the parabola as a function of temperature. It neither predicts the change of D_0 as a function of temperature, nor does it account for the dependence of the partition coefficients on additional variables like composition of melts and crystals in multicomponent systems. Looking at the parabolas of this study (Fig. 2) it must be kept in mind that melt composition changes considerably (Table 3) by raising the temperature from 800°C to 900°C. It is well documented in the literature that partition coefficients vary significantly as a function of the ratio between the number of nonbridging oxygens and the number of tetrahedrons (NBO/T) (Mysen and Virgo, 1980; Ewart and Griffin, 1994; Kohn and Schofield, 1994; Gaetani and Grove, 1995).

To assess the effect of melt composition, NBO/T-ratios have been recalculated for liquid compositions obtained in this study using the method outlined in Mysen et al. (1982). The procedure was modified by Nielsen (1985, 1988) who pointed out that it is inadequate to assign Al entirely as a network former. As a consequence of this, the Ca-activity of peraluminous melts becomes zero, which is inconsistent with the precipitation of Ca-rich clinopyroxenes or amphiboles from these melts. He proposed that only that part of Al that is charge-balanced by the alkalis acts as network former. The water present in the melts of our study causes another problem. Water may be dissolved in silicate

liquids as H_2O and OH^- (Wasserburg, 1957; Shaw, 1964; Stolper, 1982), but the latter species only acts as a network modifier. As there is no reliable way to predict the proportion of OH^- present in our melts, we completely ignored this species as a network modifier. As a consequence the NBO/T values shown in Fig. 4 are minimal values. However, this does not affect the conclusions drawn. With total water contents ranging from 9 to 12.5 wt.%, the proportion of OH^- in our melts at temperatures from 800°C to 900°C cannot be very different. It may therefore be inferred that the partition coefficients are negatively correlated with NBO/T (Fig. 4), indicating that the partition coefficients increase with the degree of polymerization of the melt.

The dependence of the partition coefficients on melt composition can be eliminated, if the *D*-values are expressed as the ratio D^* of the fraction of a cation on the M2- or M4-site in amphibole and the mole fraction of that cation related to the total of network modifiers in the melt. The remaining variations of D^* may then be attributed to temperature variations, because (1) amphiboles do not change their composition, and (2) pressure is identical in all runs. As shown in Section 5.1, the temperature dependence of partition coefficients of a series of isovalent cations entering the same lattice site may be expressed by that of D_0. To distinguish between effects of melt composition and temperature we have calculated values of D_0^* for the tri- and tetravalent cations of this study. In Fig. 5 their logarithms are related by a linear function to the reciprocal temperature. Values calculated for andesitic systems (Green and Pearson, 1985; Brenan et al., 1995) plot on the extension of the function in Fig. 5, whereas the data for basanitic systems (Adam and Green, 1994; LaTourette et al., 1995) generally do not. Large variations of D_0^* between the values of Adam and Green (1994) at the same temperature may be due to changes in pressure, as suggested by these authors.

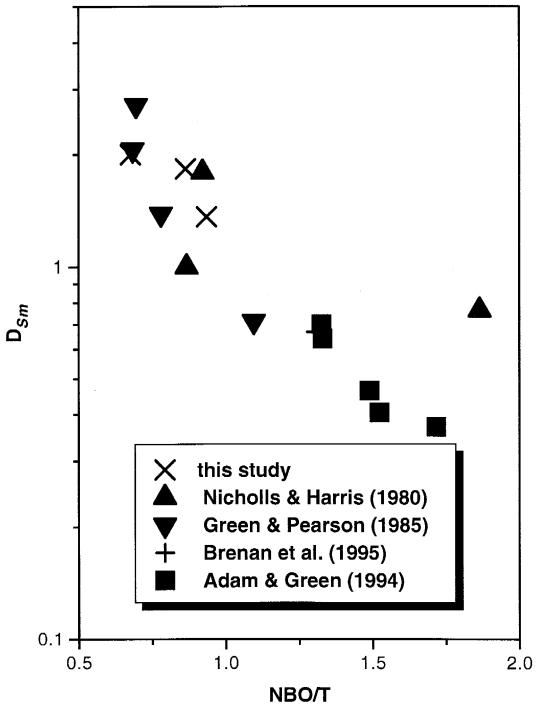

Fig. 4. Correlation between the partition coefficients and the degree of polymerization of the melt expressed as NBO/T at temperatures from 800°C-900°C.

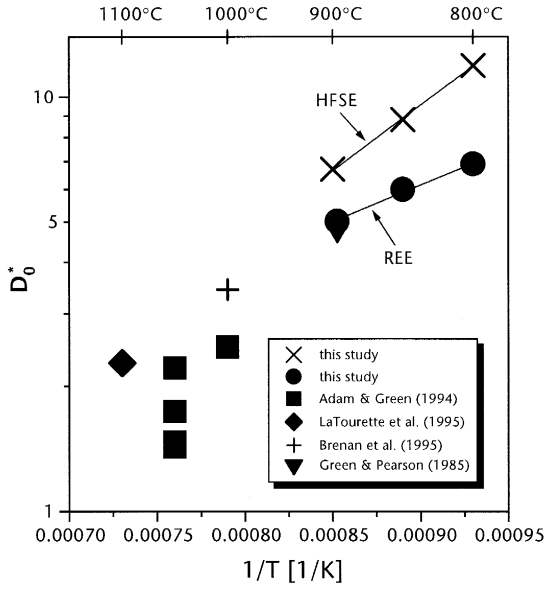

Fig. 5. Correlation between the partition coefficients, normalized to the degree of depolymerisation of the melt (for explanation see text), and the temperatures of experiments for a wide range of starting compositions (tonalites, andesites, basanites) at different temperatures (800°C-1150°C). Experimental conditions of the literature data: Adam and Green (1994): 1000°C-1100°C, 0.5-2 GPa; Brenan et al. (1995): 1000°C, 1.5 GPa; LaTourette et al. (1995): 1100°C, 1.5 GPa; Nicholls and Harris (1980): 900°C-1020°C, 1 GPa; Green and Pearson (1985): 900°C-1050°C, 0.75-2 GPa.

5.4. Correlations between partition coefficients of major and trace elements

For clinopyroxenes it is well documented that the REE partition coefficients correlate with those of Ti (Gallahan and Nielsen, 1992; Hack et al., 1994). Such a correlation holds true also for amphiboles as observed in our study. As an example (Fig. 6), we have chosen Sm because the largest sets of experimentally determined data exist for this element (Nicholls and Harris, 1980; Green and Pearson, 1985; Adam and Green, 1994; Sisson, 1994; Brenan et al., 1995). In spite of the large compositional variations of the systems studied (basanites, andesites, dacites, rhyolites, and tonalites), most data plot on a line.

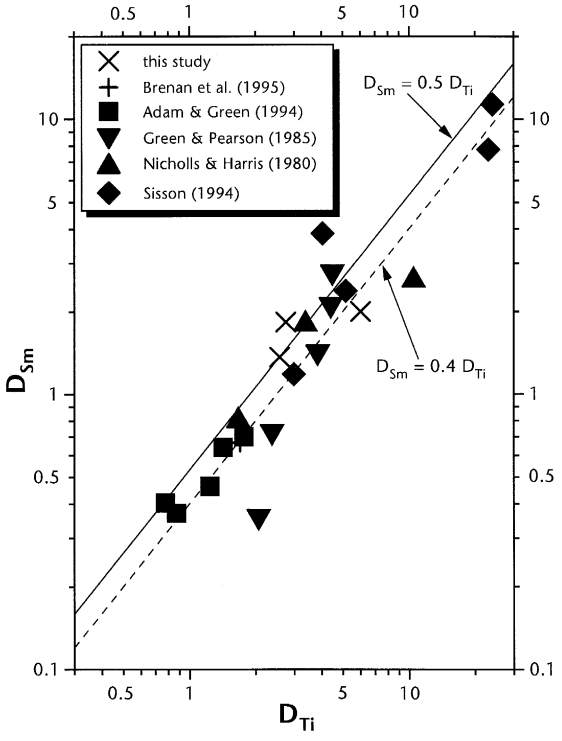

Fig. 6. Correlation between the partition coefficients of the REE and Ti for experiments on a wide range of starting compositions (tonalites, andesites, basanites) at different temperatures (800°C-1150°C). Solid and dashed lines are calculated from the parabola parameters fitted from the 900°C and 800°C data of this study. Experimental conditions of the literature data: Adam and Green (1994): 1000°C-1100°C, 0.5-2 GPa; Brenan et al. (1995): 1000°C, 1.5 GPa; Green and Pearson (1985): 900°C–1050°C, 0.75–2 GPa; Nicholls and Harris (1980): 900°C–1020°C, 1 GPa.

Gallahan and Nielsen (1992) and Hack et al. (1994) suggested that the correlations between D_{REE} and D_{Ti} are caused by the Al activity in the melt which itself may affect D_{Ti} and D_{REE} in the same way.

However, at least in our case this correlation is more readily explained using the Blundy and Wood (1994) model: if we divide Eq. (1) for D_{Sm} by that for D_{Ti} we obtain Eq. (3).

$$D_{Sm} = \frac{D_0^{REE}}{D_0^{HFSE}} \times \exp\left\{ -\frac{4\pi N_A}{RT}\left(E^{REE}\left[\frac{r_0^{REE}}{2}\left(r_{Sm} - r_0^{REE}\right)^2 + \frac{1}{3}\left(r_{Sm} - r_0^{REE}\right)^3 \right] - E^{HFSE}\left[\frac{r_0^{HFSE}}{2}\left(r_{Ti} - r_0^{HFSE}\right)^2 + \left(r_{Ti} - r_0^{HFSE}\right)^3 \right] \right) \right\} \times D_{Ti} \quad (3)$$

At a given temperature D_0, E and r_0 are constant. Hence, Eq. (3) in coordinates of D_{Sm} and D_{Ti} is a straight line passing through the origin. Its slope is determined by the product of the exponential term and D_0^{REE}/D_0^{HFSE}. Lines calculated for 800°C and 900°C by substituting the fitted parameters from Table 5 into Eq. (3) are presented in Fig. 6. The differences in slope and position due to temperature are small. Consequently, within analytical uncertainties, a nearly linear relationship between both partition coefficients is to be expected. In addition, the calculated curves agree very well with the experimentally or empirically determined partitioning data of the literature.

In an analogous way correlations between D_{REE} and D_{Ca} can be evaluated (Fig. 7); such correlations have been reported before by Sisson (1994) and Klein (1995). Due to the lack of partition coefficients of other divalent cations we can fit E and D_0 for the divalent cations only by relying on the method outlined for estimating the fraction of Eu^{2+} in Section 5.2. Then straight-line relationships between the partition coefficients of Sm and Ca can be calculated. As shown in Fig. 7, again the differences between lines corresponding to 800°C (dashed line) and 900°C (solid line) are small. The slopes for 800°C (0.8) and 900°C (0.7) are close to the results of Sisson (1994) who reported values of 1.0. On the other hand,

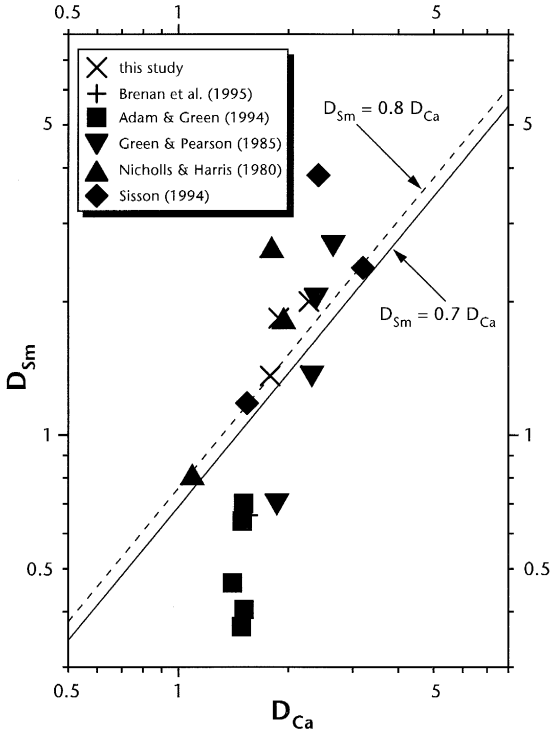

Fig. 7. Correlation between the Sm and Ca partition coefficients for experiments on a wide range of starting compositions (tonalites, andesites, basanites) at different temperatures (800°C-1150°C). Solid and dashed lines are calculated from the parabola parameters fitted from the 900°C and 800°C data of this study. Experimental conditions of the data of the literature: Adam and Green (1994): 1000°C-1100°C, 0.5-2 GPa; Brenan et al. (1995): 1000°C, 1.5 GPa; Nicholls and Harris (1980): 900°C-1020°C, 1 GPa; Green and Pearson (1985): 900°C-1050°C, 0.75-2 GPa.

experimental partitioning data for basanitic (Adam and Green, 1994) and some andesitic systems (Brenan et al., 1995) plot off the calculated lines. This may be ascribed to differences in the ratios of D_0^{REE}/D_0^{2+} between amphiboles grown from strongly alkalic and intermediate magmas.

6. Conclusions

We have shown that experimental amphibole/liquid REE and HFSE partitioning data are well accounted for by the elastic moduli model of Blundy and Wood (1994). The algorithm of Blundy and Wood (1994) predicts partition coefficients $D^{Xt/L}$ for suites of isovalent cations at given temperatures as a function of their ionic radii. It does not allow to calculate partition coefficients as a function of chemical variables X^L and X^S which themselves depend on temperature. Using the melt structure model of Nielsen (1985, 1988) we are able to distinguish between temperature and compositional effects on D and show that partition coefficients $D^{amph/L}$ correlate linearly with reciprocal temperature. As a consequence of nearly identical values of Young's moduli E and lattice sites geometries of M4- and M2-site in amphibole and clinopyroxene, respectively, the partition coefficient ratios D^{Amph}/D^{Cpx} for all REE are identical and hence the REE patterns of Cpx's and Amph's will be subparallel. Provided that E, r_0 and one partition coefficient of the suite of divalent cations are known, the partition coefficient for Eu^{2+} and, consequently, the Eu^{2+}/Eu^{3+} ratios may be estimated from Eu-bulk partition coefficients in amphibole/melt equilibria. On the basis of the fitted parabola parameters for the REE, HFSE and divalent cations, calculated straight-line relationships between D_{REE} and D_{Ca} as well as between D_{REE} and D_{Ti} agree very well with experimentally and empirically determined data of the literature (Nicholls and Harris, 1980; Green and Pearson, 1985; Adam and Green, 1994; Sisson, 1994; Brenan et al., 1995) and this study. Our Amph/L partitioning data, together with yet unpublished data for Cpx/L and Gnt/L partitioning are relevant to test models of tonalite genesis. Such modelling indicates that amphibolites low in garnet are inadequate source rocks. A further paper will be devoted to discuss these questions of tonalite petrogenesis.

Acknowledgements

We wish to thank J. Craven and R. Hinton for their forbearance and kind help with the ion-microprobe analyses. In addition, the guidance of N. Shimizu at the Woods Hole ion probe was essential in evaluating Henry's Law behaviour. We thank K.H. Wedepohl for providing sample T1 used as our starting composition. Special thanks are due to D.B. Dingwell at the Bayerisches Geoinstitut for the production of the glass of sample T1. Constructive

reviews by R.L. Nielsen, T. Rushmer and T.W. Sisson helped to improve the paper. This study was supported by a grant from the DFG within the priority research programme 'Experimental studies on element partitioning in geologically relevant systems' for which we are grateful.

References

Adam, J., Green, T.H., 1994. The effects of pressure and temperature on the partitioning of Ti, Sr, and REE between amphibole, clinopyroxene, and basanitic melts. Chem. Geol. 117, 219–233.

Adam, J., Green, T.H., Sie, S.H., 1993. Proton microprobe determined partitioning of Rb, Sr, Ba, Y, Zr, Nb and Ta between experimentally produced amphiboles and silicate melts with variable F content. Chem. Geol. 109, 29–49.

Arth, J.G., Barker, F., 1976. Rare-earth partitioning between hornblende and dacitic liquid and implications for the genesis of trondhjemitic–tonalitic magmas. Geology 4, 534–536.

Beard, J.S., Lofgren, G.E., 1991. Dehydration melting and water-saturated melting of basaltic and andesitic greenstones and amphibolites at 1, 3 and 6.9 kb. J. Petrol. 32, 365–401.

Blundy, J., Wood, B., 1994. Prediction of crystal-melt partition coefficients from elastic moduli. Nature 372, 452–454.

Bohlen, S.R., Essene, E.J., Boettcher, A.L., 1980. Reinvestigation and application of olivine quartz orthopyroxene barometry. Earth Planet. Sci. Lett. 47, 1–10.

Boyd, F.R., Finger, L.W., Chayes, F., 1969. Computer reduction of electron probe data. Carnegie Inst. Washington Yearb. 67, 210–215.

Brenan, J.M., Shaw, H.F., Ryerson, F.J., Phinney, D.L., 1995. Experimental determination of trace-element partitioning between pargasite and a synthetic hydrous andesitic melt. Earth Planet. Sci. Lett. 135, 1–11.

Chazot, G., Menzies, M.A., Harte, B., 1996. Determination of partition coefficients between apatite, clinopyroxene, amphibole, and melt in natural spinel lherzolites from Yemen: Implications for wet melting of the lithospheric mantle. Geochim. Cosmochim. Acta 60, 423–437.

Comodi, P., Mellini, M., Ungaretti, L., Zanazzi, P.F., 1991. Compressibility and high pressure structure refinement of tremolite, pargasite and glaucophane. Eur. J. Mineral. 3, 485–499.

Deming, W.E., 1964. Statistical Adjustment of Data. Dover Publications, 261 pp.

Ewart, A., Griffin, W.L., 1994. Application of proton-microprobe data to trace-element partitioning in volcanic rocks. Chem. Geol. 117, 251–284.

Gaetani, G.A., Grove, T.L., 1995. Partitioning of rare earth elements between clinopyroxene and silicate melt: crystal–chemical controls. Geochim. Cosmochim. Acta 59, 1951–1962.

Gallahan, W.E., Nielsen, R.L., 1992. The partitioning of Sc, Y, and the rare earth elements between high-Ca pyroxene and natural mafic to intermediate lavas at 1 atmosphere. Geochim. Cosmochim. Acta 56, 2387–2404.

Green, T.H., Pearson, N.J., 1985. Experimental determination of REE partition coefficients between amphibole and basaltic to andesitic liquids at high pressure. Geochim. Cosmochim. Acta 49, 1465–1468.

Green, T.H., Adam, J., Sie, S.H., 1992. Trace element partitioning between silicate minerals and carbonatite at 25 kbar and application to mantle metasomatism. Mineralogy and Petrology 46, 179–184.

Hack, P.J., Nielsen, R.L., Johnston, A.D., 1994. Experimentally determined rare-earth element and Y partitioning behaviour between clinopyroxene and basaltic liquids at pressures up to 20 kbar. Chem. Geol. 117, 89–105.

Hart, S.R., Dunn, T., 1993. Experimental cpx/melt partitioning of 24 trace elements. Contrib. Mineral. Petrol. 113, 1–8.

Hauri, E.H., Wagner, T.P., Grove, T.L., 1994. Experimental and natural partitioning of Th, U, Pb and other trace elements between garnet, clinopyroxene and basaltic melts. Chem. Geol. 117, 149–166.

Hazen, R.M., Finger, L.W., 1979. Bulk modulus–volume relationship for cation–anion polyhedra. J. Geophys. Res. 84, 6723–6728.

Hinton, R.W., Harte, B., 1995. Ion probe measurements of National Institute of Standards and Technology standard reference material SRM 610 glass, trace elements. Analyst 120, 1315–1319.

Johannes, W., 1973. Eine vereinfachte Piston–Zylinder-Apparatur hoher Genauigkeit. Neues Jahrb. Mineral., 7/8: 337–351.

Johnson, K.T.M., Dick, H.J.B., Shimizu, N., 1990. Melting in the oceanic upper mantle: A ion microprobe study of diopsides in abyssal peridotites. J. Geophys. Res. 95, 2661–2678.

Klein, M., 1995. Experimentelle Bestimmung von Kristall/Schmelze-Verteilungskoeffizienten ausgewählter Spurenelemente für Klinopyroxene, Granate und Amphibole. Implikationen für die Genese tonalitischer Magmen. Dr. rer. nat. thesis, Univ. Köln, 182 pp.

Kohn, S.C., Schofield, P.F., 1994. The importance of melt composition in controlling trace element behaviour: an experimental study of Mn and Zn partitioning between forsterite and silicate melts. Chem. Geol. 117, 57–71.

LaTourette, T., Hervig, R.L., Holloway, J.R., 1995. Trace element partitioning between amphibole, phlogopite, and basanite melt. Earth Planet. Sci. Lett. 135, 13–30.

Leake, B.E., 1978. Nomenclature of amphiboles. Mineral. Mag. 42, 533–563.

McKay, G.A., Seymour, R.J., 1982. Electron microprobe analysis of trace elements in minerals at 10 ppm concentrations. In: K. Heinrich (Editor), Microbeam Analysis, Proc. 17th Annu. Conf. Microbeam Anal. Soc. San Francisco Press, pp. 431–434.

Mysen, B.O., Virgo, D., 1980. Trace element partitioning and melt structure: an experimental study at 1 atm pressure. Geochim. Cosmochim. Acta 44, 1917–1930.

Mysen, B.O., Virgo, D., Seifert, F.A., 1982. The structure of silicate melts—implications for chemical and physical properties of natural magma. Rev. Geophys. Space Phys. 20, 353–383.

Nicholls, I.A., Harris, K.L., 1980. Experimental rare earth element

partition coefficients for garnet, clinopyroxene and amphibole coexisting with andesitic and basaltic liquids. Geochim. Cosmochim. Acta 44, 287–308.

Nielsen, R.L., 1985. A method for the elimination of the compositional dependence of trace element distribution coefficients. Geochim. Cosmochim. Acta 49, 1775–1779.

Nielsen, R.L., 1988. A model for the simulation of combined major and trace element liquid lines of descent. Geochim. Cosmochim. Acta 52, 27–38.

Rapp, R.P., 1995. Amphibole-out phase boundary in partially melted metabasalt, its control over liquid fraction and composition, and source permeability. J. Geophys. Res. 100, 15601–15610.

Rapp, R.P., Watson, E.B., 1995. Dehydration melting of metabasalt at 8–32 kbar: implications for continental growth and crust–mantle recycling. J. Petrol. 36, 891–931.

Rapp, R.P., Watson, E.B., Miller, C.F., 1991. Partial melting of amphibolite/eclogite and the origin of Archean trondhjemites and tonalites. Precambrian Res. 51, 1–25.

Reed, S.J.B., 1975. Electron Microprobe Analysis. Cambridge Monographs on Physics. Cambridge University Press, 400 pp.

Rudnick, R.L., Taylor, S.R., 1986. Geochemical constraints on the origin of Archean tonalitic–trondhjemitic rocks and implications for lower crustal composition. In: J.B. Dawson, D.A. Carswell, J. Hall and K.H. Wedepohl (Editors), The nature of the lower continental crust. Geol. Soc. Spec. Publ. 24, 179–191.

Rushmer, T., 1991. Partial melting of two amphibolites: contrasting experimental results under fluid-absent conditions. Contrib. Mineral. Petrol. 107, 41–59.

Shannon, R.D., Prewitt, C.T., 1968. Effective ionic radii in oxides and fluorides. Acta Crystallogr. 25B, 925–946.

Shaw, H.R., 1964. Theoretical solubility of H_2O in silicate melts: quasi-crystalline models. J. Geol. 72, 601–617.

Shimzu, N., LeRoex, A.P., 1986. The chemical zoning of augite phenocrysts in alkaline basalts from Gough Island, South Atlantic. J. Volcanol. Geotherm. Res. 29, 159–188.

Sisson, T.W., 1991. Pyroxene–high silica rhyolite trace element partition coefficients measured by ion microprobe. Geochim. Cosmochim. Acta 55, 1575–1585.

Sisson, T.W., 1994. Hornblende-melt trace element partitioning measured by ion microprobe. Chem. Geol. 117, 331–344.

Skulski, T., Minarik, W., Watson, E.B., 1994. High-pressure experimental trace-element partitioning between clinopyroxene and basaltic melts. Chem. Geol. 117, 127–147.

Stolper, E.M., 1982. Water in silicate glasses: an infrared spectroscopic study. Contrib. Mineral. Petrol. 81, 1–17.

Streckeisen, A., LeMaitre, R.W., 1979. A chemical approximation to the modal QAPF classification of igneous rocks. Neues Jahrb. Mineral. Abh. 136, 169–206.

Sweeney, R.J., Green, D.H., Sie, S.H., 1992. Trace and minor element partitioning between garnet and amphibole and carbonatitic melt. Earth Planet. Sci. Lett. 113, 1–14.

Wasserburg, G.J., 1957. The effect of H_2O in silicate systems. J. Geol. 65, 15–23.

Wedepohl, K.H., Heinrichs, H., Bridgwater, D., 1991. Chemical characteristics and genesis of the quartz-feldspathic rocks in the Archean crust of Greenland. Contrib. Mineral. Petrol. 107, 163–179.

Winther, K.T., Newton, R.C., 1991. Experimental melting of hydrous low-K tholeiite: evidence on the origin of Archean cratons. Bull. Geol. Soc. Den. 39, 213–228.

Witt-Eickschen, G., Harte, B., 1994. Distribution of trace elements between amphibole and clinopyroxene from mantle peridotites of the Eifel (western Germany): an ion-microprobe study. Chem. Geol. 117, 235–250.

Wolf, M.B., Wyllie, P.J., 1994. Dehydration-melting of amphibolite at 10 kbar: the effects of temperature and time. Contrib. Mineral. Petrol. 115, 369–383.